Three-Level BDDC for Virtual Elements

Axel Klawonn, Martin Lanser, and Adam Wasiak

1 Introduction

The Virtual Element Method (VEM) is a Galerkin-type method for the solution of partial differential equations which allows for the discretization with general polygonal/polyhedral meshes. Furthermore, the VEM framework allows for the relatively simple construction of trial and test spaces with desirable properties on these general meshes. In recent years, numerous variants of the VEM have been proposed and analyzed, which include nonconforming, high-regularity, high-order, and hourglass-stabilized variants [4, 5, 9, 11]. The different approaches have been applied to many different model problems. As a framework to make the VEM suitable for large scale problems, the FETI-DP (Finite Element Tearing and Interconnecting - Dual Primal) and BDDC (Balancing Domain Decomposition by Constraints) domain decomposition methods have been introduced for virtual element discretizations [6, 7], which allows for an efficient and parallel iterative solution on large-scale computers. Recently, the analysis has been extended to the Stokes problem in [8], and adaptive coarse spaces for virtual element discretizations have been considered in [10] for mixed form problems in three dimensions and in [13] for stationary diffusion and linear elasticity in two dimensions. The use of adaptive coarse spaces allows for the solution of highly heterogeneous problems, for example, stationary diffusion problems with jumps in the diffusion coefficient, since, in the case of both finite and virtual elements, the method is provably robust. In [14] a condition number bound of the preconditioned system which only depends on geometrical constants and a user defined tolerance was shown for finite element discretizations and in [13]

Axel Klawonn, Martin Lanser
Department of Mathematics and Computer Science, Division of Mathematics, University of Cologne, Weyertal 86-90, 50931 Cologne, Germany and Center for Data and Simulation Science, University of Cologne, Germany, e-mail: axel.klawonn@uni-koeln.de, martin.lanser@uni-koeln.de

Adam Wasiak
Department of Mathematics and Computer Science, Division of Mathematics, University of Cologne, Weyertal 86-90, 50931 Cologne, Germany, e-mail: adam.wasiak@uni-koeln.de

the same was shown for the virtual element case. Unfortunately, adaptive coarse spaces can be large, especially for decompositions with many subdomains and/or difficult coefficient distributions. Also, classical coarse spaces grow proportionally with the number of subdomains and, in a parallel context, with the number of parallel resources. These large global coarse problems are a typical parallel scalability bottleneck in BDDC and FETI-DP methods, since the exact solution using, for example, sparse direct solvers does not scale. To alleviate this difficulty in BDDC, numerous multilevel approaches have been proposed, where the solution of the coarse problem is approximated by applying BDDC recursively using a very coarse domain decomposition. This allows for a parallel solution of the coarse problem and thus improves scalability. Here, we consider the three-level BDDC preconditioner introduced in [16] and apply it to the BDDC method with virtual element discretizations for the first time.

2 Model problems and the virtual element method

The domain $\Omega \subset \mathbb{R}^2$ is assumed to be a polygon. Let $f \in L^2(\Omega)$. We consider the stationary diffusion equation with homogeneous Dirichlet boundary values

$$-\nabla \cdot (\rho \nabla u) = f \quad \text{in } \Omega, \qquad u = 0 \quad \text{on } \partial\Omega.$$

Here, we assume ρ to satisfy $0 < \rho_* \leq \rho(x) \leq \rho^*$ for two constants $\rho_*, \rho^* \in \mathbb{R}$. The corresponding weak formulation is given by

$$\begin{cases} \text{Find } u \in H^1_0(\Omega) \text{ such that} \\ a(u,v) = (f,v)_{L^2(\Omega)} \text{ for all } v \in H^1_0(\Omega), \end{cases} \tag{1}$$

where $a(v,w) := (\rho \nabla v, \nabla w)_{L^2(\Omega)}$ for $v, w \in H^1_0(\Omega)$. We briefly introduce the VEM as it is presented in [2, 1]. Let $\{\mathcal{T}_h\}_h$ be a sequence of quasi-uniform tessellations of Ω into a finite number of simple polygons K, where $h := \max_{K \in \mathcal{T}_h} h_K$ and $h_K := \operatorname{diam}(K)$. Each polygon has a finite number of vertices. Let $\mathbb{P}_k(K)$ denote the space of polynomials of at most degree k on K. The meshes are assumed to satisfy the following condition. There exists a $\gamma > 0$ such that for all h and for all $K \in \mathcal{T}_h$:

1. K is star-shaped with respect to a ball of radius $\geq \gamma h_K$.
2. The distance between any two vertices of K is $\geq \gamma h_K$.

Denoting the set of edges of K by $\mathcal{E}^K$ and defining $\mathbb{P}_{-1} = \{0\}$, a suitable local virtual element space for the target order of accuracy $k \in \mathbb{N}$ is given by

$$V^h(K) = \{v \in H^1(K) \colon v|_e \in \mathbb{P}_k(e)\, \forall e \subset \mathcal{E}^K,\ v|_{\partial K} \in C(\partial K),\ \Delta v \in \mathbb{P}_{k-2}(K)\},$$

where $C(\partial K)$ denotes the continuous functions on the boundary of K. Then the global virtual element space can be defined as $V^h = \{v \in H^1_0(\Omega) \colon v|_K \in V^h(K)\}$. We can choose the following degrees of freedom on V^h:

- The values of v_h on each polygon vertex.
- For $k \geq 2$, the $k-1$ values of v_h on each point of the Gauss-Lobatto quadrature rule on every edge of the tessellation.
- For $k \geq 2$ and all $K \in \mathcal{T}_h$, the volume moments up to order $k-2$ of v_h in K.

The term $a(u_h, v_h)$ cannot be computed for $v_h, w_h \in V^h$ from the given degrees of freedom. Therefore, we replace $a(\cdot,\cdot)$ with a suitable approximate bilinear form $a_h(\cdot,\cdot)$ obtaining the discrete variational problem: Find $u_h \in V^h$ such that $a_h(u_h, v_h) = f_h(v_h)\ \forall v_h \in V^h$. For more details on the construction and implementation of $a_h(\cdot,\cdot)$ and related theoretical estimates we refer to [1, 2, 3].

3 BDDC and three-level BDDC

Let us give a brief description of the BDDC method as it applies to virtual element discretizations. Let $\{\Omega_i\}_{i=1}^N$ be a nonoverlapping domain decomposition of Ω such that $\overline{\Omega} = \cup_{i=1}^N \overline{\Omega}_i$, equipped with sequences of quasi-uniform tessellations $\mathcal{T}_i^h$, $i = 1, ..., N$ that satisfy the VEM grid assumptions. For each subdomain Ω_i, we obtain local stiffness matrices $K^{(i)}$ and load vectors $f^{(i)}$ using the VEM.

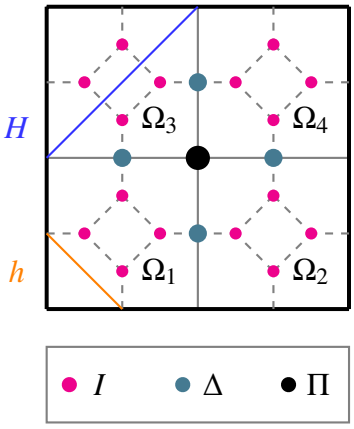

Fig. 1 Domain decomposition with polygonal meshes.

We denote by H_i the diameter of Ω_i and define $H := \max_i H_i$. Let $\Gamma := \cup_{i \neq j} \partial\Omega_i \cap \partial\Omega_j \backslash \partial\Omega_D$ be the interface, that is, the set of all points that belong to at least two subdomains. Further denoting by Γ_h the set of all degrees of freedom (d.o.f.) which lie on the interface, we split these into two distinct sets, the set of primal degrees of freedom (Π) and the set of dual degrees of freedom (Δ) obtaining $\Gamma_h = \Delta \cup \Pi$. In this article, the primal variables are chosen as the subdomain vertices. For degrees of freedom in the interior, we use the index I. A depiction can be found in Fig. 1. Finally, we require the decomposition to be conforming, that is, the virtual element nodes coincide on the interface. We denote the local discrete virtual element spaces $V^h(\Omega_i) := V^h \cap H^1(\Omega_i)$. We further define the local discrete trace spaces $W_i := V^h(\partial\Omega_i \cap \Gamma_h)$ and let $W := \prod_{i=1}^N W_i$.

3.1 Standard BDDC

The BDDC method is defined as follows. We assume the following local ordering of the degrees of freedom which yields the following representation of the decomposed stiffness matrices, solution vectors, and right-hand sides

$$K = \begin{bmatrix} K_{II} & K_{I\Gamma} \\ K_{\Gamma I} & K_{\Gamma\Gamma} \end{bmatrix}, \qquad u = \begin{bmatrix} u_I \\ u_\Gamma \end{bmatrix}, \qquad \text{and} \qquad f = \begin{bmatrix} f_I \\ f_\Gamma \end{bmatrix},$$

where $K_{II} := \operatorname{diag}_{i=1}^{N} K_{II}^{(i)}$ and $K_{I\Gamma} := \operatorname{diag}_{i=1}^{N} K_{I\Gamma}^{(i)}$. In the same way, we have $u_I^T = (u_I^{(1)T}, \dots, u_I^{(N)T})$, and similarly for u_Γ, f_I, and f_Γ. We define the unassembled Schur complement and the reduced right-hand side by

$$S := S_{\Gamma\Gamma} = K_{\Gamma\Gamma} - K_{\Gamma I} K_{II}^{-1} K_{I\Gamma} \qquad \text{and} \qquad \mathrm{g} := \mathrm{g}_\Gamma = \mathrm{f}_\Gamma - \mathrm{K}_{\Gamma\mathrm{I}} \mathrm{K}_{\mathrm{II}}^{-1} \mathrm{f}_\mathrm{I}.$$

We denote by $R_\Pi^T = (R_\Pi^{(1)T}, R_\Pi^{(2)T}, \dots, R_\Pi^{(N)T})$ and $R_\Delta^T = (R_\Delta^{(1)T}, R_\Delta^{(2)T}, \dots, R_\Delta^{(N)T})$ the partial finite element assembly operators with values in $\{0, 1\}$, which assemble the system in the primal variables. We further define $R_\Gamma = \operatorname{diag}(R_\Delta, I_\Pi)$.

By assembling S and g in the primal variables we obtain

$$\widetilde{S} = \begin{bmatrix} I_\Delta & \\ & R_\Pi^T \end{bmatrix} S \begin{bmatrix} I_\Delta & \\ & R_\Pi \end{bmatrix} =: \begin{bmatrix} S_{\Delta\Delta} & \widetilde{S}_{\Delta\Pi} \\ \widetilde{S}_{\Pi\Delta} & \widetilde{S}_{\Pi\Pi} \end{bmatrix} \qquad \text{and} \qquad \widetilde{g} = \begin{bmatrix} I_\Delta & \\ & R_\Pi^T \end{bmatrix} g.$$

By assembling these systems in the dual variables we obtain the standard BDDC system

$$R_\Gamma^T \widetilde{S} R_\Gamma u_g = R_\Gamma^T \widetilde{g} \quad \Longleftrightarrow: \quad S_g u_g = g_g.$$

Next, we introduce scaling matrices $D^{(i)}$ belonging to their subdomains Ω_i. Consider the domain Ω_i which shares the edges $\mathcal{E}^{ij_1}, \dots, \mathcal{E}^{ij_n}$ with the subdomains $\Omega_{j_1}, \dots, \Omega_{j_n}$, respectively. Ordering $D^{(i)}$ according to the edges, yields $D^{(i)} = \operatorname{diag}_{m=1}^{n} D_{\mathcal{E}^{ijm}}^{[i]}$. We further require that the two scaling matrices belonging to an interface edge $\mathcal{E}^{ij}$ satisfy $D_{\mathcal{E}^{ij}}^{[i]} + D_{\mathcal{E}^{ij}}^{[j]} = I$, where I denotes the identity matrix. Here, we consider ρ-scaling [15]. With these scaling matrices, the scaled versions of R_Δ and R_Γ are defined as $R_{D,\Delta}^T = (R_{D,\Delta}^{(1)T}, \dots, R_{D,\Delta}^{(N)T})$ and $R_{D,\Gamma} = \operatorname{diag}(R_{D,\Delta}, I_\Pi)$, where $R_{D,\Delta}^{(i)} = D^{(i)} R_\Delta^{(i)}$. Finally the preconditioned BDDC system is given by

$$M^{-1} S_g u_g = M^{-1} g_g, \qquad \text{where} \qquad M^{-1} := M_{\mathrm{BDDC}}^{-1} := R_{D,\Gamma}^T \widetilde{S}^{-1} R_{D,\Gamma}.$$

4 Three-level BDDC

The three-level BDDC method is now characterized by an approximate solution of the linear Schur complement system $\widetilde{S} z = r$ which occurs in the preconditioner and thus has to be solved in each iteration for an arbitrary residual vector r. The approximation is based on a recursive application of the two-level BDDC preconditioner to the coarse problem using a coarser third level decomposition for the set of primal degrees of freedom. More precisely, the exact inverse $\widetilde{S}_{\Pi\Pi}^{-1}$ is replaced by the BDDC preconditioner on the third level within each application of $\widetilde{S}^{-1}$. We define the

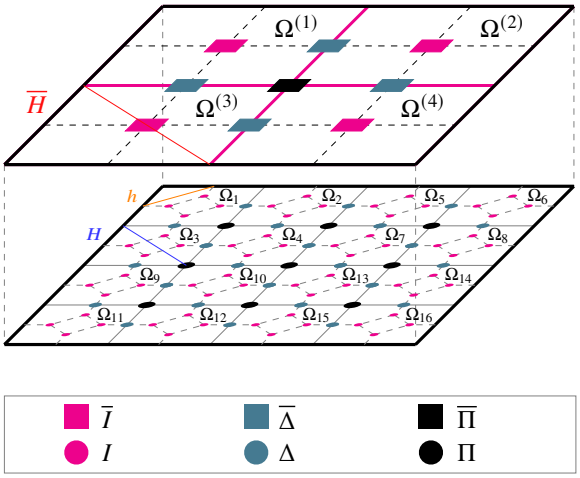

Fig. 2 Example of a three-level domain decomposition into 16 regular subdomains (bottom) and 4 regular subregions (top) with polygonal meshes on the subdomains. The interface $\overline{\Gamma}$ between subregions is marked in magenta.

operator $\widehat{S}$ such that the solution of $\hat{z} = \widehat{S}^{-1}r$ is the desired approximation of z and we will discuss its construction below. This allows us to define the three-level preconditioner

$$M_{3\mathrm{L}}^{-1} := R_{D,\Gamma}^T \widehat{S}^{-1} R_{D,\Gamma}.$$

We decompose Ω into N subregions $\Omega^{(j)}$ with diameters $\overline{H}$. Each subregion is the union of N_j subdomains, which we will denote by $\Omega_i^{(j)}$, $i = 1, \ldots, N_j$. To create a third level, we split the primal variables Π into different categories, just as in the two level case. Let $\overline{\Gamma} \subset \Pi$ be the interface between the subregions, that is, the primal variables belonging to two or more subregions. We further split the subregion interface into dual and primal variables obtaining $\overline{\Gamma} = \overline{\Delta} \cup \overline{\Pi}$. Here, the subregion primal variables are those that are connected to three or more subregions, that is, the vertices of the subregions. The remaining primal variables are denoted as $\overline{I}$. An example of a three-level decomposition is shown in Fig. 2. The operator $\widehat{S}$ is constructed by applying BDDC to the subregion decomposition. Instead of assembling the global Schur complement on all primal variables, the third-level decomposition is used to assemble a Schur complement on each subregion. For these subregion Schur complements, the BDDC preconditioner is built analogously to the second level and replaces the inverse action of $\widetilde{S}_{\Pi\Pi}^{-1}$ in each iteration of BDDC. In general (under certain assumptions on the coefficient distribution), the resulting system requires more PCG iterations to converge to the desired tolerance and shows higher condition numbers than the classical BDDC method but is more efficient due to being able to be computed in parallel. For more details we refer to [12, 16].

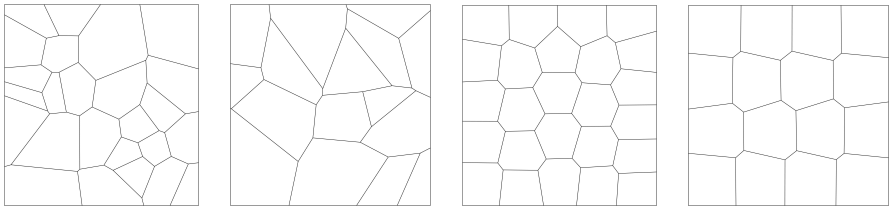

Fig. 3 Voronoi tessellations (two figures on the left) and Centroidal Voronoi Tessellations (CVT) (two figures on the right) with 25 and 16 elements respectively used for the numerical experiments.

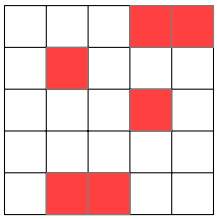

BDDC			Three-level BDDC					
			$\overline{H}/H = 5,\ H/h \approx 5$			sr $= 5 \times 5,\ \overline{H}/H = 5$		
H/h	it	cond	sr	it	cond	$\overline{H}/H$	it	cond
≈ 25	15	2.38	5×5	21	4.09	5	21	4.09
≈ 50	16	2.40	10×10	25	4.73	10	24	5.12
≈ 75	16	2.40	15×15	26	4.90	15	28	6.43

Fig. 4 Condition numbers (cond) and iteration numbers (it) for BDDC and three-level BDDC with linear virtual element discretizations for a stationary diffusion problem. The coefficient distribution and the decomposition in subregions (sr) for the third level in the case of 5×5 subregions are shown on the left side. The Voronoi tessellation with 25 elements shown in Fig. 3 is used on each subdomain. The coefficient function is 10^6 on the red patches and 1 on the white ones.

5 Numerical results

For the numerical experiments, we consider $\Omega = [0,1]^2$ and regular domain decompositions into $m \times m$ quadratic subdomains and $M \times M$ quadratic subregions. To create a conforming decomposition, the meshes in Fig. 3 are mirrored across the subdomain interface. The PCG method is iterated until a relative reduction of the residual of 10^{-8} is reached. The results in Fig. 4 confirm the expected behavior of BDDC and three-level BDDC for the case of virtual elements, where using the three-level variant increases the iteration numbers and condition numbers slightly. Nonetheless, the method is fairly robust and scalable against increasing the number of subregions or their size. This is comparable to the finite element case. Similar results can be obtained for CVT meshes. Considering a subregion checkerboard pattern as the coefficient distribution, both meshtypes, and virtual elements of order $k = 1, 2$ in Table 1, we can observe a similar behavior.

To conclude, we have applied the three-level BDDC method to virtual element discretizations. The method shows a similar performance to its finite element counterpart. A proof of the three-level BDDC condition number bound to virtual element discretizations is in preperation.

Table 1 Condition numbers (cond) and iteration numbers (it) for three-level BDDC with virtual element discretizations with polynomial degree given by k for a coefficient distribution in a subregion (sr) checkerboard pattern with a contrast of 10^6. The subdomain meshes for $H/h \approx 5$ and $H/h \approx 4$ are shown in Fig. 3.

$\overline{H}/H = 5,\ H/h \approx 5$				
$k = 1$	Voronoi		CVT	
sr	it	cond	it	cond
5×5	14	2.33	13	2.33
10×10	14	2.33	13	2.33
15×15	14	2.35	13	2.35

sr $= 5 \times 5,\ H/h \approx 5$				
$k = 1$	Voronoi		CVT	
$\overline{H}/H$	it	cond	it	cond
5	14	2.33	13	2.33
10	15	2.38	14	2.38
15	15	2.39	14	2.39

sr $= 5 \times 5,\ \overline{H}/H = 5$				
$k = 1$	Voronoi		CVT	
H/h	it	cond	it	cond
≈ 5	14	2.33	14	2.33
≈ 10	17	3.19	17	3.22
≈ 15	19	3.65	19	3.76

$\overline{H}/H = 4,\ H/h \approx 4$				
$k = 2$	Voronoi		CVT	
sr	it	cond	it	cond
4×4	17	3.53	16	3.55
8×8	17	3.54	16	3.55
12×12	17	3.54	16	3.55

sr $= 4 \times 4,\ H/h \approx 4$				
$k = 2$	Voronoi		CVT	
$\overline{H}/H$	it	cond	it	cond
4	17	3.53	16	3.55
8	18	3.53	18	3.57
12	19	3.56	18	3.60

sr $= 4 \times 4,\ \overline{H}/H = 4$				
$k = 2$	Voronoi		CVT	
H/h	it	cond	it	cond
≈ 4	17	3.53	16	3.55
≈ 8	20	4.49	20	4.44
≈ 12	21	4.66	22	5.64

References

1. Ahmad, B., Alsaedi, A., Brezzi, F., Marini, L. D., and Russo, A. Equivalent projectors for virtual element methods. *Computers & Mathematics with Applications* **66**(3), 376 – 391 (2013).
2. Beirão da Veiga, L., Brezzi, F., Cangiani, A., Manzini, G., Marini, L. D., and Russo, A. Basic principles of virtual element methods. *Mathematical Models and Methods in Applied Sciences* **23** (2012).
3. Beirão da Veiga, L., Brezzi, F., Marini, L. D., and Russo, A. The hitchhiker's guide to the virtual element method. *Mathematical Models and Methods in Applied Sciences* **24**(08), 1541–1573 (2014).
4. Beirão da Veiga, L., Dassi, F., and Russo, A. High-order virtual element method on polyhedral meshes. *Computers & Mathematics with Applications* **74**(5), 1110–1122 (2017). SI: SDS2016 - Methods for PDEs.
5. Beirão da Veiga, L. and Manzini, G. A virtual element method with arbitrary regularity. *IMA Journal of Numerical Analysis* **34**(2), 759–781 (2013).
6. Bertoluzza, S., Pennacchio, M., and Prada, D. BDDC and FETI-DP for the virtual element method. *Calcolo* **54**, 1565–1593 (2017).
7. Bertoluzza, S., Pennacchio, M., and Prada, D. FETI-DP for the three dimensional virtual element method. *SIAM Journal on Numerical Analysis* **58**(3), 1556–1591 (2020).
8. Bevilacqua, T. and Scacchi, S. BDDC preconditioners for divergence free virtual element discretizations of the Stokes equations. *Journal of Scientific Computing* **92**(2) (2022).
9. Cangiani, A., Manzini, G., Russo, A., and Sukumar, N. Hourglass stabilization and the virtual element method. *International Journal for Numerical Methods in Engineering* **102**(3-4), 404–436 (2015).
10. Dassi, F., Zampini, S., and Scacchi, S. Robust and scalable adaptive BDDC preconditioners for virtual element discretizations of elliptic partial differential equations in mixed form. *Computer Methods in Applied Mechanics and Engineering* **391**, 114620 (2022).
11. de Dios, B. A., Lipnikov, K., and Manzini, G. The nonconforming virtual element method. *ESAIM: Mathematical Modelling and Numerical Analysis* **50**(3), 879–904 (2016).

12. Klawonn, A., Lanser, M., Rheinbach, O., and Weber, J. Preconditioning the coarse problem of BDDC methods - three-level, algebraic multigrid, and vertex-based preconditioners. *ETNA - Electronic Transactions on Numerical Analysis* **51**, 432–450 (2019).
13. Klawonn, A., Lanser, M., and Wasiak, A. Adaptive and frugal FETI-DP for virtual elements. *Vietnam Journal of Mathematics* (2022).
14. Klawonn, A., Radtke, P., and Rheinbach, O. A comparison of adaptive coarse spaces for iterative substructuring in two dimensions. *Electron. Trans. Numer. Anal.* **45**, 75–106 (2016).
15. Klawonn, A., Widlund, O. B., and Dryja, M. Dual-primal FETI methods for three-dimensional elliptic problems with heterogeneous coefficients. *SIAM Journal on Numerical Analysis* **40**(1), 159–179 (2002).
16. Tu, X. Three-level BDDC in two dimensions. *International Journal for Numerical Methods in Engineering* **69**(1), 33–59 (2007).